Reaction Rates in Fractal vs. Uniform Catalysts with Linear and Nonlinear Kinetics

C. Gavrilov and M. Sheintuch
Dept. of Chemical Engineering, Technion, Haifa, Israel, 32000

Pore fractal objects are expected to be optimal catalysts, since material is supplied to the narrower pores, which are also shorter through the larger pores where diffusion resistance is smaller. To demonstrate this, diffusion and reaction were simulated on Sierpinski-gasket-type fractal objects and on the corresponding nonfractal uniform-pore structures of the same size, porosity and reactive area. Positive order reactions limited by Knudsen diffusion were shown to exhibit larger rates in fractal than in uniform-pore objects. Fractal catalysts also exhibited a new intermediate domain in which the rate depends only weakly on the kinetics parameters. In nonmonotonic kinetics the branching point (bifurcation point) was extremely sensitive to the pore structure.

Introduction.

The problems of reaction and diffusion in a fractal catalyst have recently attracted considerable attention (e.g. see articles that Giona et al., 1996, Coppens and Froment, 1996, Mougin et. al., 1996 presented at the recent ISCRE meeting). Problems of reaction and diffusion are core problems in reaction engineering, but for years they have been modeled with effective parameters that depend mainly on the porosity and surface area of the structure. Modeling of the pore network by random structures and the critical phenomena of percolation was the subject of investigations in the 1980's (Sahimi, 1988; Sahimi et al., 1990). The interest in fractal porous structures, as models for real catalysts stems from the novelty of the structure as well as from the large amount of experimental evidence that many porous solids show scaling that indicates fractality (Avnir et al., 1985, Rothschild, 1991). Also, models of solid aggregation that produce fractal structures resemble preparation methods of certain porous materials (Elias-Kochav et. al., 1991).

Branching porous catalyst should be optimal for reaction and diffusion purposes in a way similar to that of the lungs or blood vessels: the narrow pores, where the effective diffusivity is small due to small cross sections or to Knudsen diffusivity, are also the shorter pores, and the corresponding Thiele modulus is moderate. The narrow pores are supplied by longer but larger pores where the effective diffusivity is greater. In the present work, we test these optimal features by computing and comparing the average rate in ordered fractal and nonfractal catalysts with linear or nonlinear kinetics. We show that, indeed, for positive order kinetics a fractal catalyst is superior to its uniform counterpart. This superiority is especially evident in the Knudsen diffusion regime where the diffusivity is proportional to the pore width, while the difference in rate is small in the molecular-diffusion regime.

Two fractal structures (Sierpinski gaskets), whose pores have different aspect ratios are considered: in a gasket with wide two-dimensional pores the concentration field is two-dimensional and a two-dimensional grid of unit-size elements is required for solving the problem. This approach cannot work with catalysts with many generations, since we are limited by the maximal size of the grid that can be considered. Also, the porosity of such objects is high (above 0.9), well beyond that found in commercial catalysts. In a gasket with narrow pores the network can be described as a set of pores of different sizes. A one-directional concentration gradient can be assumed in each pore and can be solved as a function of its end-point concentrations. Thus, the concentration values at the pore crossings can be determined by the flux balances for all crossings. Such a model accounts for the geometrical structure of the porous network and allows the solution for an object with a large number of generations to be calculated because it is not limited by the size of the object but only by the numbers of pores per side.

Several approaches have been applied to determine the overall rate and scaling behavior of fractal porous catalysts since the problem was formulated by Sheintuch and Brandon (1989). The simpler approach is to calculate the effective properties (density, void fraction, tortuosity, surface area) and their space dependence based on the scaling properties of

the catalyst (Sheintuch and Brandon, 1989; Coppens and Froment, 1994, 1995, 1996). This approach applies to mass fractals (e.g., DLA objects formed by diffusion-limited aggregation), and typically shows that under diffusion limitations the properties close to the boundary determine the overall rate. In a similar approach Yang et al. (1987) compared the rates of uni- and bimolecular reactions on circular aggregates and DLA clusters and found that DLA aggregates showed faster dynamics.

Another possible approach is to solve exactly the reaction–diffusion problem on a well-defined, ordered pore network. A series of works has been devoted to solving the problem of first-order reaction and diffusion in a porous branching fractal object that does not contain closed loops. The object can take the form of a branching pore-tree, where branches bifurcate from the trunk (Sheintuch and Brandon, 1989) or of a Mandelbrot Lung, where smaller branches bifurcate from the end of the previous branch (Aris, 1991), or of a Devil's comb (Mougin et al., 1996), which is quite similar to the pore tree. Analytical results for the effectiveness factor can be obtained by solving each pore individually and the whole structure iteratively. A new asymptote in the plot of log(*rate*) vs. log(k) was found for such objects using approximate solutions (Sheintuch and Brandon, 1989) or numerical methods (Mougin et al., 1996). The new asymptote, which lies between the known asymptotes of slopes 1 (reaction control) and 0.5 (diffusion control), is of a smaller slope. Giona et al. (1996) recently used input/output renormalization and Green function formalism to obtain exact recursion for the effectiveness factor for a first-order reaction in a generally ordered fractal porous catalyst with one input node. They obtained a new asymptote, which applies under certain geometrical constraints, and scales as rate $\alpha\, k^{1-D_f/D_w}$, where D_w is the dimension of random walks. Since the value of D_w is not known for the structure under study here, and since not all geometrical constants apply to our structure, we cannot validate this asymptote.

Numerical solutions for a first-order reaction and diffusion in stochastic structures like DLA, CCA (cluster–cluster–aggregation), and random objects were considered by Elias-Kochav et al. (1991) in order to relate the properties of the solid to its preparation methods. Other works have dealt with transport properties in a fractal pore (see e.g., Giona and Roman, 1992; Giona et al., 1995), and diffusion toward and reaction on fractal surfaces (Gutfraind and Sheintuch, 1992).

The works just reviewed considered pore networks with open loops and linear kinetics controlled mainly by molecular diffusion. Most real porous catalysts, however, would be systems with closed loops and the catalytic kinetics are typically nonlinear. Also, Knudsen diffusion applies for transport in the narrower pores of real objects. These features are the subject of the present work and, as we show, it is in this regime that the fractal structure is superior to the uniform one.

Objects with Two-Dimensional Pores

Methodology

A five-generation Sierpinski gasket (Figure 1) was used as a two- dimensional object with two-dimensional pores in the simulation of diffusion and first order reaction. The gasket cross section is a Cantor set with a common self-similarity ratio of 1/3. The problem was stated in a square (243 by 243) grid, where the solid is denoted by full cells and void by empty cells. The transient problem of diffusion and first order reaction is generally described by

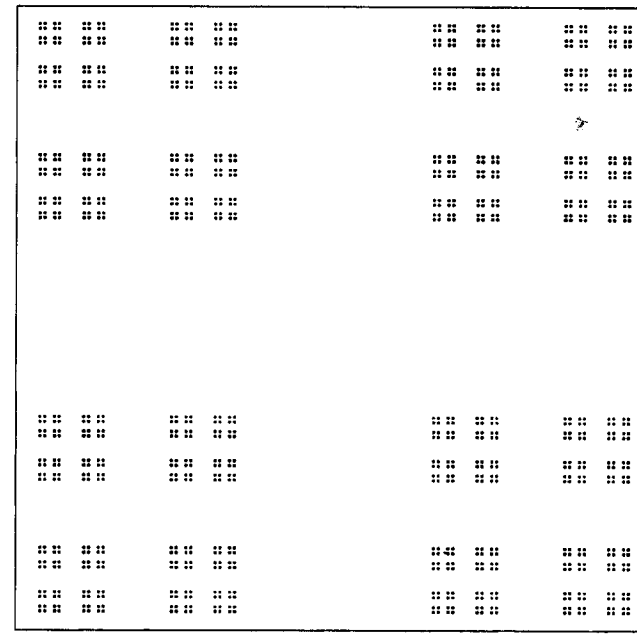

Figure 1. Five-generation Sierpinski gasket with 2-D pores for reaction-diffusion simulations.
Concentration was set to unity at its boundaries.

$$\frac{\partial C}{\partial t} = D\nabla^2 C - ks(x,y)C, \tag{1}$$

subject to the boundary condition $C = 1$ at the outer border. The rate constant and the diffusivity were distributed in space: in Eq. 1 k is the rate constant per unit interface and $s(x, y)$ is the active-area distribution; reaction was assumed to occur only at the void–solid interface. Diffusion applied only to empty cells, and the diffusivity D was assumed constant (equal to unity) in the case of molecular diffusion and proportional to the pore size in the case of Knudsen diffusion, when for the pores of generation i it was computed as

$$D_{Kn} = 3^{i-5}, \tag{2}$$

so that $D = 1$ at the largest pores ($i = 5$) and it declines with pore size. The steady-state solution was determined by solving the transient problem stated in a finite difference form using one-point cells: at each integration step of duration (δt), the concentration in the cell (i, j) was updated according to

$$\delta C(i,j) = \frac{D}{4}\left\{\Sigma(i,j) - [4 - p(i,j)]C(i,j) - 4p(i,j)\frac{kC(i,j)}{D}\right\}\delta t, \tag{3}$$

where $p(i, j)$ is the number of interface borders for cell (i, j) ($p = 0$, 1, or 2) and $\Sigma(i, j)$ is the sum of concentrations in the

adjacent void cells. The boundary condition was introduced as

$$C(0,j) = C(i,0) = C(244,j) = C(i,244) = 1. \qquad (4)$$

After a sufficiently long time the solution converged to the steady state of the original problem.

Results

The concentration fields for the moderate diffusion resistance case show the expected behavior (Figure 2; colors denote the concentration with a resolution of 1/64): diffusion resistance is smaller in the larger pores and the field follows the catalyst density distribution. In the case of Knudsen diffusion, the concentration field shows distinct self-similarity as evident from the blowup (Figure 2b) of the lower left corner of the field (Figure 2a). In the case of molecular diffusion (Figure 2c, 2d), however, the fields were self-similar only for larger values of the reaction constant.

Reaction rates on the fractal gasket were compared with those on a pseudohomogeneous catalyst—an object of the same size, porosity and reactive area, for which all parameters of the system were lumped into one model,

$$\nabla^2 C = \Phi_{ef}^2 C; \quad \Phi_{ef} = \sqrt{\frac{k_{ef} L^2}{D_{ef}\epsilon}}, \qquad (5a)$$

for which an analytical solution exists. Here ϵ is the porosity of the catalyst; effective diffusivity D_{ef} was equal to unity in the case of molecular diffusion and was $1/\bar{R}$ in the case of Knudsen diffusion, where $\bar{R}$ is the pore size of the uniform-pore analog of the fractal catalyst, which is the object with the same porosity and the same interface area. Effective rate constant k_{ef} and $\bar{R}$ were computed as

$$k_{ef} = 4k\left(1 - \epsilon\frac{\sqrt{1-\epsilon}}{L}\right) \approx 4k(1-\epsilon), \qquad (5b)$$

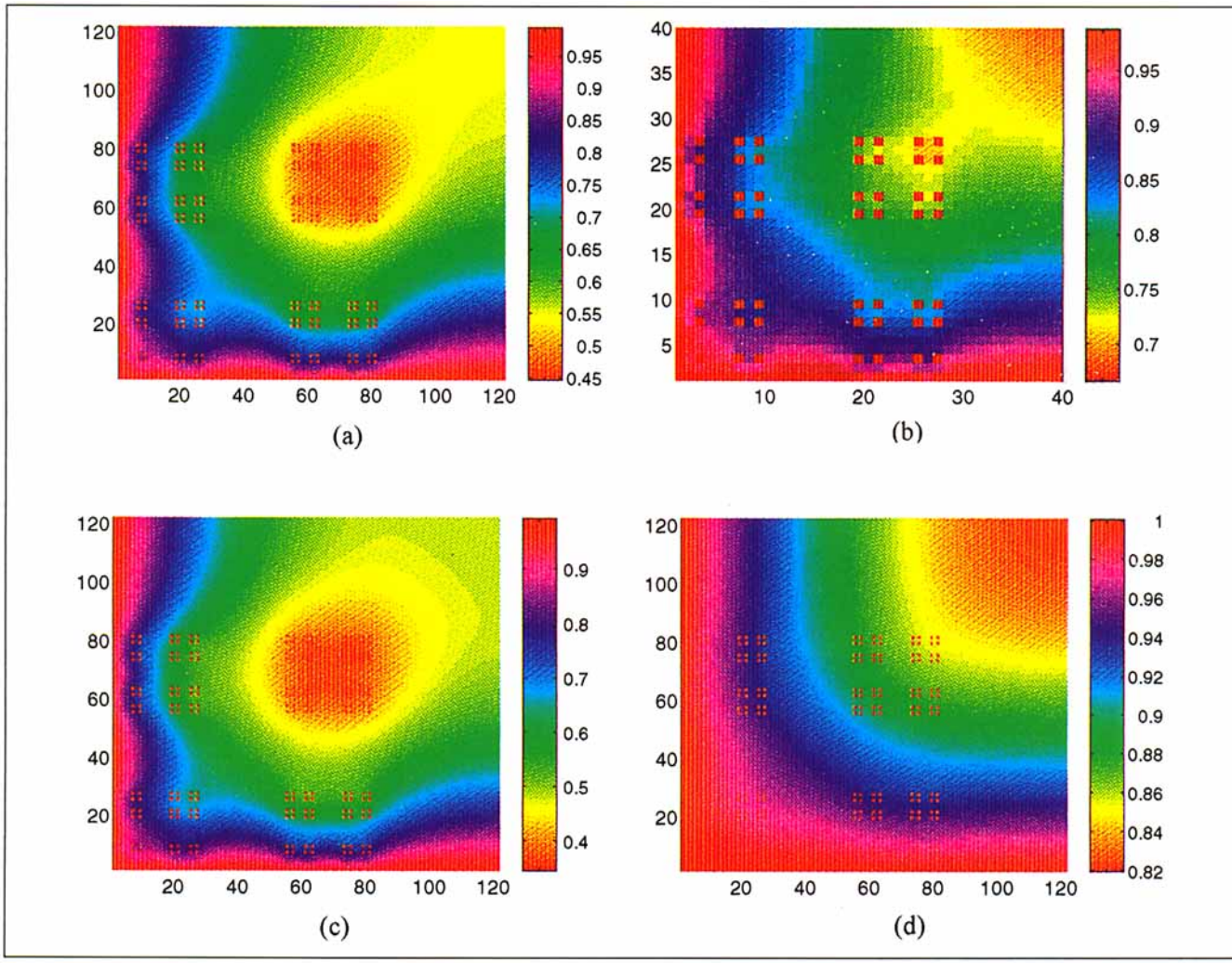

Figure 2. Typical concentration fields in the object of 2-D pores (Figure 1) with Knudsen (a), (b) and molecular (c), (d) diffusion.

It shows one quadrant with $k = 1.22e-4$ (a), $k = 7.81e-3$ (c) and $k = 2.44e-4$ (d); subplot (b) shows a blowup of left bottom corner for (a).

$$\bar{R} = \left(\frac{1-\sqrt{1-\epsilon}}{\sqrt{1-\epsilon}-1/L} \right) \approx \frac{1}{\sqrt{1-\epsilon}} - 1. \qquad (5c)$$

Despite the distinct self-similarity of concentration fields, the fractal catalyst showed no gain in reaction rates over that of the pseudohomogeneous model in either the Knudsen or the molecular diffusion case. This is expected, since the porosity of the fractal gasket employed in the simulation is high (around 0.9), and consequently diffusion resistance is not significant. This result is expected to hold for nonlinear kinetics. The porosity values of real catalysts are usually in the range of 0.4–0.6. In order to obtain a gain in reaction rates we have to consider fractal catalysts with lower porosities. Solving the reaction–diffusion problem in such objects with a two-dimensional grid is very difficult, even on powerful computers, due to enormous memory requirements, and consequently we had to resort to a solid model of one-dimensional pores.

Linear Kinetics in Objects with 1-D Pores

Methodology

Now we consider an object with a reasonable porosity, a Sierpinski gasket with narrow pores (Figure 3a). Its cross sections are still Cantor sets with each segment containing two openings of size R_0; the aspect ratio of the pores can be easily determined, and for the simulations below it was chosen to be 0.1. Since the aspect ratio of these pores is small, we assume a one-dimensional concentration gradient along each pore. The object was described as a set of pore units. For each unit the reaction rate was determined to be a function of the concentrations of its end points. Using a one-unit solution, a steady state condition was written for each pore intersection requiring that the sum of fluxes entering it must be equal to zero. The flux balances on the intersections reduced the system to a set of unknowns that represent the values of the concentration at the intersections. Symmetry of the object was used to effectively reduce the number of unknowns by solving only one octant of the original solid model. This octant formed a triangle AOB (Figure 3a) with one side exposed to a fixed concentration ($C = 1$) and the other two sides subject to symmetry conditions ($\partial C/\partial n = 0$, where n is normal to the side). The obtained system of equations was solved by a linear solver (Matlab 4.2), and the resulting solution was used to build the concentration field and compute the reaction rate.

Simulations of objects with four or five generations, for linear or nonliner kinetics and with Knudsen or molecular diffusion, were performed. The same simulations were repeated for a non-fractal uniform-pore catalyst (Figure 3b) of the same size, porosity, number of pores per side and reactive area as those of the fractal object.

We now develop the solution for a single-pore unit of length L_{ab} and width R_{ab} connecting nodes a and b (Figure 4): the diffusion-reaction problem in the node is described by (with $n = 1$):

$$R_{ab} D_{ab} \frac{d^2C}{dx^2} = 2kC^n, \qquad (6)$$

subject to $C(x = 0) = C_a$, $C(x = l_{ab}) = 2kC_b$. Diffusivity D_{ab} is set to R_0/R_{ab} in the Knudsen-diffusion case (where R_0 is the width of the largest pore) or to 1 in the molecular diffusion case.

In dimensionless form the solution for Eq. 6 is

$$C(x^*) = C_a \cosh(\Phi_{ab} x^*) + \frac{C_b - C_a \cosh(\Phi_{ab})}{\sinh(\Phi_{ab})} \sinh(\Phi_{ab} x^*), \qquad (7)$$

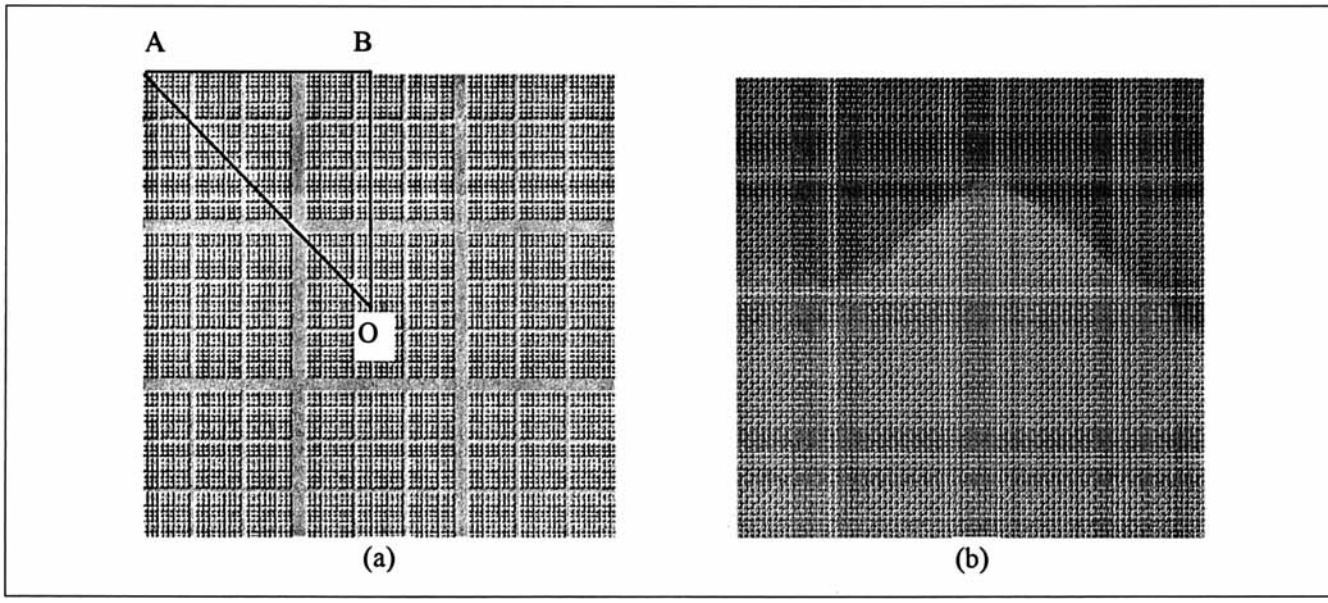

Figure 3. Sierpinski gasket with one-dimensional pores used as a model of fractal catalyst (a) and the uniform-pore catalyst employed for comparison (b).

Both objects have the same porosity, reactive area, and number of pores per side.

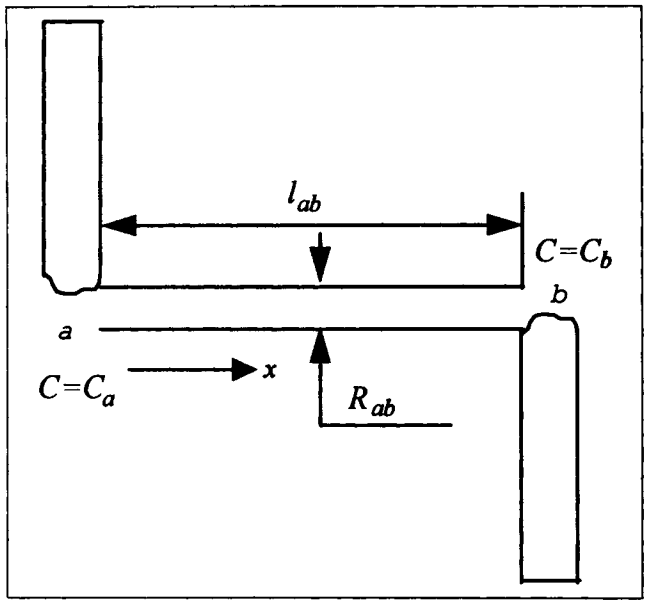

Figure 4. Single pore connecting nodes *a* and *b*.

where the Thiele modulus Φ_{ab} and coordinate x^* are given by

$$\Phi_{ab} = \sqrt{\frac{2k}{D_{ab}R_{ab}}}\, l_{ab}, \quad x^* = x/l_{ab}. \tag{8}$$

The expression for the flux at end b in the direction of x becomes

$$J_b = -D_{ab}R_{ab}\left.\frac{dC}{dx}\right|_{x=l_{ab}} = \sqrt{2kD_{ab}R_{ab}} \times \left[\frac{C_a}{\sinh(\Phi_{ab})} - \frac{C_b}{\tanh(\Phi_{ab})}\right], \tag{9}$$

and the expression for the reaction rate in one unit becomes

$$\text{Rate}_{ab} = \Phi_{ab}^2 D_{ab}\int_0^1 C(x^*)\,dx^* = \Phi_{ab}D_{ab}\tanh(0.5\Phi_{ab})(C_a + C_b). \tag{10}$$

the total reaction rate can then be computed as

$$\text{Rate}_\Sigma = \sum_{a,b}\text{Rate}_{ab} = \sum_{a,b}\Phi_{ab}D_{ab}\tanh(0.5\Phi_{ab})(C_a + C_b), \tag{11}$$

where summation is done over all units. To find C_a, C_b, the sum of fluxes on all nodes is equated to zero, forming a system of 820 or 7,361 linear algebraic equations for an object of four or five generations.

Results

The fractal catalyst showed significant gain in performance over uniform-pore catalysts in the Knudsen-diffusion regime. No significant difference was found in the molecular-diffusion regime. The concentration fields in the case of Knudsen diffusion (Figure 5) demonstrate how a fractal catalyst optimizes the diffusion flux: the wider pores, which are also characterized by a larger diffusivity, serve as channels for transport into the narrow pores that contain most of the reactive area. One can see that the inner small pores are supplied by large pores, while those at the surface are supplied directly by the surface. At low values of k the problem is two-dimensional with loops formed by intersecting pores. At large rate constants the loops can be, ignored, and the solution is very similar to that in a branching pore-tree or the Devil's comb. In a uniform-pore catalyst, on the other hand, the pores are supplied by the surface and there is no optimization of the flux (Figure 5). The gain in rates over the uniform-pore object reached 70% in the catalyst with four generations (Figure 6a, 6b) and 134% in the catalyst with five generations (Figure 6c, 6d). Fractal catalysts also show an intermediate low-slope domain in the plot of (log)*rate* vs. (log)k, which connects the known asymptotes of kinetic control (slope 1) and diffusion control (slope 1/2) (Figure 6a, 6c). This intermediate domain was observed using simulations of other kinetics as well, and we will return to discuss its features in the concluding remarks. In the molecular diffusion case, fractal catalysts showed the same performance as uniform-pore catalysts (Figure 6e).

Positive-(Second and Third) Order Kinetics

Although resistance to diffusion is independent of concentration at all pore levels for first order kinetics, the resistance in reactions of order $n > 1$ increases with concentration and thus, resistance will be larger at the outer (and larger) pores. To study the effect of reaction order, we considered the problems of second- and third-order reactions with Knudsen diffusion in a five-generations fractal catalyst and in its uniform-pore analog.

Methodology

The solution method was similar to that employed for the linear problem, except that in the solution for the single pore unit we linearized the rate expression around the average concentration in the pore (actually, at the previous iteration; the first iteration employed the linear-kinetics solution). The problem for pore-section connecting nodes a, b is defined by Eq. 6. Its linearized analog is

$$D_{ab}\frac{d^2C}{dx^2} = \frac{2k}{R_{ab}}[(1-n)C_{ab}^{*n} + nC_{ab}^{*n-1}C], \tag{12}$$

where C_{ab}^* is the average concentration in the pore (a, b). Its solution is given by Eq. 7 with $C(x^*)$ substituted by $C(x^*)+\alpha$, and so on:

$$C(x^*)+\alpha = (C_a+\alpha)\cosh(\Phi_{ab}x^*) + \frac{(C_b+\alpha)-(C_a+\alpha)\cosh(\Phi_{ab})}{\sinh(\Phi_{ab})}\sinh(\Phi_{ab}x^*), \tag{13}$$

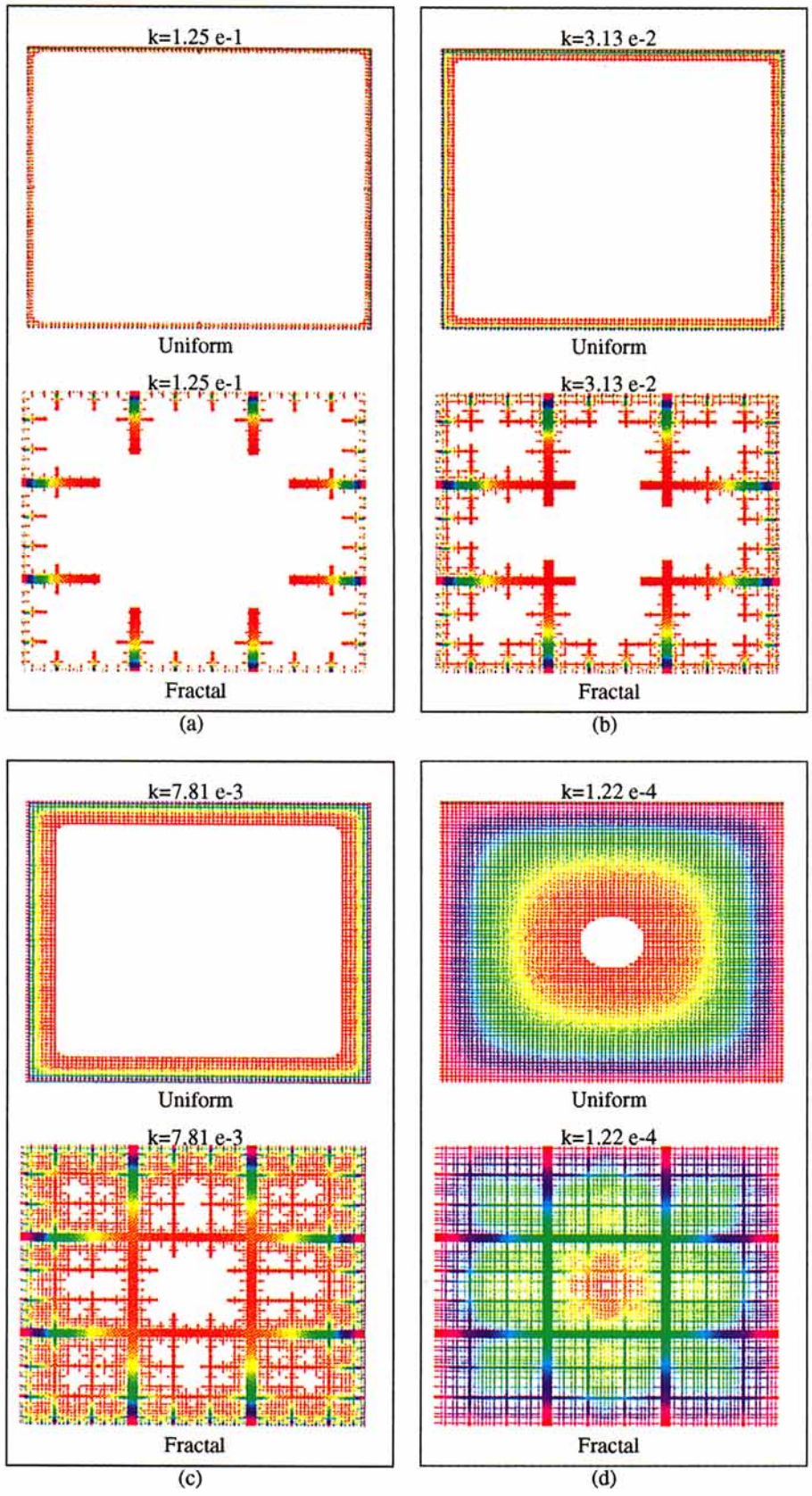

Figure 5. Samples of concentration fields in the fractal and uniform-pore objects in the case of Knudsen diffusion (linear kinetics, four generations).

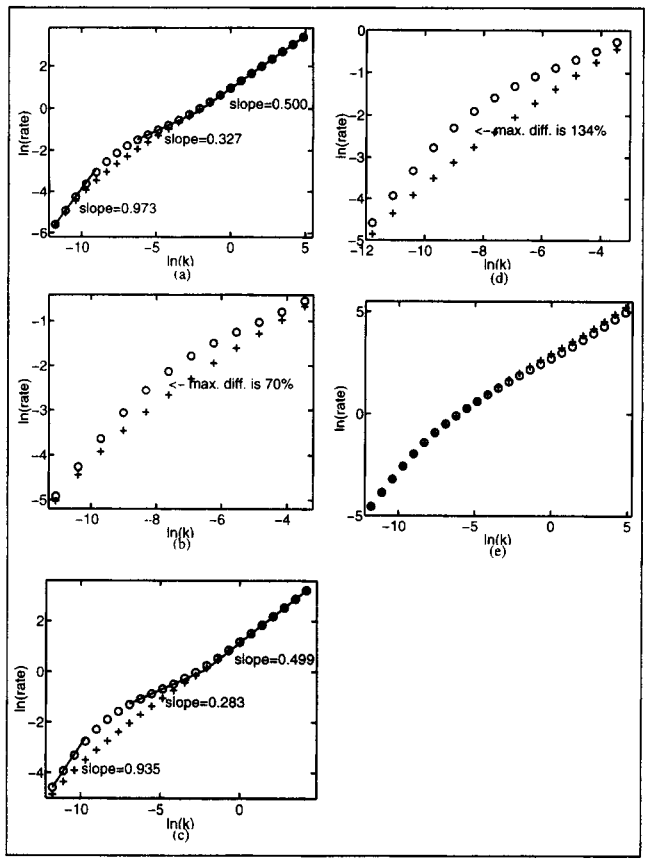

Figure 6. Comparison of rates and the asymptotic slopes in the uniform-pore (+) and fractal (o) catalyst of four (a, b) and five (c, d) generations for the case of linear kinetics and Knudsen (a)-(d) or molecular (e) diffusion.

Plots (a) and (c) show full range of simulated k, (b) and (d) show the range of intermediate asymptote.

where

$$\Phi_{ab} = \sqrt{\frac{2knC_{ab}^{*n-1}}{D_{ab}R_{ab}}}\, l_{ab}, \quad \alpha = \frac{1-n}{n} C_{ab}^{*}. \tag{14}$$

The expression for the flux at end b and rate becomes

$$J_b = -D_{ab}R_{ab}\left.\frac{dC}{dx}\right|_{x=l_{ab}} = \sqrt{2kD_{ab}R_{ab}}\left[\frac{C_a+\alpha}{\sinh(\Phi_{ab})} - \frac{C_b+\alpha}{\tanh(\Phi_{ab})}\right], \tag{15}$$

$$\text{Rate}_{ab} = \Phi_{ab}D_{ab}\tanh(0.5\Phi_{ab})(C_a + C_b + 2\alpha). \tag{16}$$

Equations 13 and 16 were used to compute the concentration profiles and reaction rates. The computation was repeated until the difference between two successive iterations became sufficiently small.

Results

The solution is quite like that in linear kinetics: the fractal catalyst showed significant improvement over the uniform-pore catalyst in second- and third-order kinetics reactions (Figure 7). The differences in rates exceeded 100% in a wide range of rate constants (several orders of magnitude). Fractal catalyst showed a new intermediate domain in the plot of log(*rate*) vs. log(k), which occurred between the known asymptotes of slope 1 and 1/2. Again, understanding this asymptote is crucial for optimizing the catalyst, since the gain in reaction rate over the uniform-pore catalyst occurred in this range. An approximate solution is necessary to characterize this asymptote and its dependence on reaction kinetics, and number of generations should be determined.

Autocatalytic Kinetics

The effect of pore structure is expected to be especially strong in autocatalytic kinetics, since such kinetics with strong diffusion resistance can admit multiple solutions. The existence boundaries of such multiplicity (the bifurcation set) are expected to be strongly dependent on diffusion resistance. To demonstrate this behavior we now simulate the reaction–diffusion problem, with rate of the form $kC(1-C)$. This rate expression is typical for processes with product acceleration like $A + C \rightarrow 2C$. With equal diffusivities of A and C one can find an invariant of the form

$$C_a + C_C = C_A^b + C_C^b, \tag{17}$$

where C_A^b and C_C^b are bulk concentrations of A and C, respectively. Without loss of generality we set $C_A^b = 1$ and $C_C^b =$

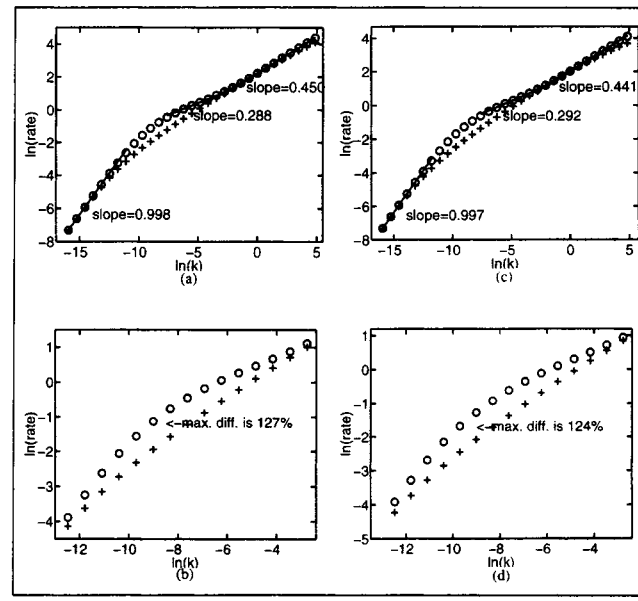

Figure 7. Comparison of rates and asymptotic slopes in the uniform-pore (+) and five generation fractal (o) catalyst for second (a), (b) and third order (c), (d) kinetics in the Knudsen diffusion regime.

Plots (a) and (c) show full range of simulated k, (b) and (d) show the range of the intermediate asymptote.

0; the rate expression for the autocatalytic system thus becomes $kC_A(1-C_A)$. We therefore solve the diffusion–reaction equation

$$D\nabla^2 C = ks(x,y)C(1-C); \quad C=1 \text{ at the boundaries,} \quad (18)$$

which always has one trivial solution ($C=1$, zero rate). This solution is stable in the region of small diffusion resistances. When this solution becomes unstable, a stable non-trivial solution emerges. The dependence of rate on k or any other parameter will have a branching point.

Methodology

The problem was solved with Knudsen diffusion on a five-generation fractal catalyst (Figure 3a) and its uniform-pore analog (Figure 3b), applying the same "nodes" method described before. When writing the equation for one pore, we linearized the rate expression around the average concentration in the same pore obtained at the preceding iteration. Hence, the linearized equation for a pore unit becomes:

$$D_{ab}\frac{d^2C}{dx^2} = \frac{2k}{R_{ab}}(C_{ab}^{*2} + (1-2C_{ab}^{*})C). \quad (19)$$

The solution is different for the cases of $C_{ab}^{*} < 1/2$ and $C_{ab}^{*} > 1/2$. In the former case, the system is described by Eqs. 13, 15, 16, with Φ_{ab} and α defined as

$$\Phi_{ab} = \sqrt{\frac{2k\,\mathrm{abs}(1-2C_{ab}^{*})}{D_{ab}R_{ab}}}\,l_{ab}, \quad \alpha = \frac{C_{ab}^{*2}}{\mathrm{abs}(1-2C_{ab}^{*})}. \quad (20)$$

When $C_{ab}^{*} > 1/2$, the concentration, flux at the end b, and reaction rate are given by

$$C(x^{*}) + \alpha = (C_a+\alpha)\cos(\Phi_{ab}x^{*}) + \frac{(C_b+\alpha)-(C_a+\alpha)\cos(\Phi_{ab})}{\sin(\Phi_{ab})}\sin(\Phi_{ab}x^{*}), \quad (21)$$

$$J_b = -D_{ab}R_{ab}\left.\frac{dC}{dx}\right|_{x=l_{ab}} = \sqrt{2kD_{ab}R_{ab}}\left[\frac{C_a+\alpha}{\sin(\Phi_{ab})} - \frac{C_b+\alpha}{\tan(\Phi_{ab})}\right], \quad (22)$$

$$\mathrm{Rate}_{ab} = \Phi_{ab}D_{ab}\tan(0.5\Phi_{ab})(C_a+C_b+2\alpha), \quad (23)$$

where Φ_{ab} and α are defined as before (Eq. 20).

Results

Both fractal and uniform-pore catalysts exhibit a bifurcation point from a trivial to a nontrivial solution (Figure 8). The k value at the branching point, however, differs by one order of magnitude. Thus, the rates ratio in fractal and uniform objects is tremendous in that region. As we have already pointed out, the fractal catalyst optimizes the diffusion resistance. In order for the nontrivial reactive state to be stable in systems with autocatalytic kinetics, the diffusion resistance should be sufficiently strong. Thus, the branching point of the reactive solution is smaller for a uniform-pore catalyst than for a fractal one. At larger values of the reaction constant, fractal catalysts demonstrate small gain (Figure 8b), as kinetics become linear in most of the catalyst volume.

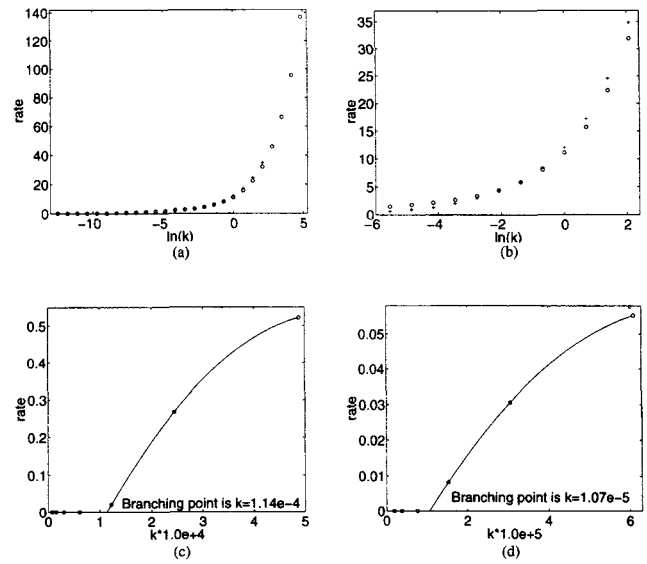

Figure 8. Comparison of rates in the uniform-pore (+) and five generation fractal (o) catalyst for autocatalytic kinetics and Knudsen diffusion: (a) full range of simulated k, (b) domain of branching, (c) branching point of fractal catalyst, (d) branching point of uniform-pore catalyst.

Concluding Remarks

Porous fractal catalysts were shown numerically to be more effective than uniform-pore objects for positive-order reactions limited by Knudsen diffusion. The ratio of rates in fractal and uniform-pore objects of four and five generations was larger than 2 in a wide range of rate constants. This superiority is achieved because the porous branching structure of a fractal catalyst provides an optimal design for reducing diffusion resistance: wider pores, where diffusion resistance is small, serve as channels for transport into the narrow pores, which have the largest amount of surface area and where diffusion resistance is strong.

In nonmonotonic kinetics that exhibit a multiplicity of solutions, the branching point in a fractal catalyst can be significantly larger than that in a uniform-pore object. This was demonstrated for the parabolic form rate $kC(1-C)$, and it occurs because the reactive solution is stable in the region of strong diffusion resistance.

Fractal objects with Knudsen diffusion show a new intermediate low-slope domain in the plot of $\log(rate)$ vs. $\log(k)$ which exists between the known asymptotes of slopes 1 and 1/2. While it is not clear whether this domain has asymptotic properties, we recall that a low-slope intermediate asymptote was predicted to exist in a pore tree of a well-defined geometry (see the Introduction). The source if this behavior is obvious: if only the smallest pores contribute to the rate, and all

the other generations are simply conduits for mass-transfer, then under diffusion-limitation conditions the rate at each generation is proportional to $\sqrt{rate}$ of the next generation of smaller pores. Thus we have total rate scales like log rate $\propto 2^{-N} \log k$, where N is the number of generations.

The Sierpinski gasket differs from the pore tree on three counts: it contains closed loops, that is, all points can be reached and supplied from the surface by several paths; it is characterized by mixed hierarchies with pores of size R_i bifurcating into pores of size R_{i+1}, R_{i+2}, ..., R_{i+n}; and, the surface supplies the main pores as well as smaller and more frequent pores. To show why the result of the pore tree applies to the gasket, note that under diffusion-control conditions the loops can be ignored, as all pores are supplied through the shortest possible path. This is evident in the concentration field that was solved for diffusion and reaction in the Sierpinski gasket (Figures 5a and 5b). The gasket can thus be viewed as a series of scaled-down pore trees that are connected to the surface, and the solution of the single large tree can be summed up for all its scaled down images to derive an approximation for the gasket. Surface supply through smaller pores becomes important under diffusion limitations, since there are more small pores than large ones. This is especially so in the case of the molecular-diffusion regime; recall that the intermediate asymptote was not observed in that case (Figure 6e). In the Knudsen-diffusion regime supply through the smaller pores is somewhat reduced since the diffusivity ($D \propto R$) is smaller. We observed that the rate in the intermediate domain scales as $k^{0.33}$ and $k^{0.28}$ for four and five generations, respectively. An approximate solution presented elsewhere suggests that, although an intermediate low-slope domain does exist for a large number of generations (N), this is not an asymptotic solution and the rate increases with N. The scaling domain width increases with N and the domain is larger for Knudsen diffusion than for molecular diffusion. Consequently, the superiority of the fractal objects may be realized at smaller k, implying a higher rates ratio in fractal and uniform-pore objects. Because of computer memory limitations the simulation could not be extended beyond five-generation objects, and we could not verify that the increase in rate computed with four and five generations will continue with more generations (N).

Two-dimensional concentration fields were calculated for the objects with very high porosity, but the solution for the effectiveness factor in this case can be described by classic approach when all parameters of the system are lumped into one effective Thiele modulus. At the same time, concentration fields demonstrate distinct self-similarity.

The suggested superiority of fractal objects opens up a whole array of processes that should be reconsidered in such objects: obviously this structure should affect the selectivity in a network of reactions in parallel or consecutive reactions. Since fractal structures reduce the diffusion resistance, we expect that fractal objects will exhibit higher selectivity for reactions of lower-order kinetics, and lower selectivity for intermediates in consecutive reactions. The problem of etching a solid porous surface or mass fractals is another application and will be considered in a future publication. Fractal objects will be less susceptible to poisoning and deactivation, since it will take longer to clog the wider diameter pores in the fractal catalyst than in a uniform-pore structure (Mougin et al., 1996).

Literature Cited

Aris, R., "Diffusion and Reaction in a Mandelbrot Lung," *Chaos Solitons Fractals*, **1**, 583 (1991).

Avnir, D., D. Farin, and P. Pfeifer, "Surface Geometric Irregularity of Particulate Materials; The Fractal Approach," *J. Colloid Interface Sci.*, **103**, 112 (1985).

Coppens, M.-O., and G. F. Froment, "Diffusion and Reaction in a Fractal Catalyst Pore: III. Application to the Simulation of Vinil Acetate Production from Ethylene," *Chem. Eng. Sci.*, **49**, 4897 (1994).

Coppens, M.-O., and G. F. Froment, "Diffusion and Reaction in a Fractal Catalyst Pore: II. Diffusion and First Order Reaction," *Chem. Eng. Sci.*, **50**, 1 (1995).

Coppens, M.-O., and G. F. Froment, "Fractal Aspects in Catalytic Reforming of Naphta," *Chem. Eng. Sci.*, **51**, 2283 (1996).

Elias-Kohav, T., M. Sheintuch, and D. Avnir, "Steady-State Diffusion and Reaction in Catalytic Fractal Porous Media," *Chem. Eng. Sci.*, **46**, 2787 (1991).

Giona, M., and H. E. Roman, "Fractional Diffusion Equation for Transport Phenomena in Random Media," *Physica A*, **185**, 87 (1992).

Giona, M., A. Adrover, and A. R. Giona, "Convection-Diffusion Transport in Disordered Structures: Numerical Analysis Based on the Exit-time Equation," *Chem. Eng. Sci.*, **50**, 1001 (1995).

Giona, M., W. A. Schwalm, A. Adrover, and M. K. Schwalm, "First Order Kinetics in Fractal Catalyst: Renormalization Analysis of Effectiveness Factor," *Chem. Eng. Sci.*, **51**, 2273 (1996).

Gutfraind, R., and M. Sheintuch, "Scaling Approach to Study Diffusion and Reaction Processes on Fractal Catalysts," *Chem. Eng. Sci.*, **47**, 4425 (1992).

Mougin, P., M. Pons, and J. Villermaux, "Reaction and Diffusion at an Artificial Fractal Interface: Evidence for a New Diffusional Regime," *Chem. Eng. Sci.*, **51**, 2293 (1996).

Rothschild, W. G., "Fractals in Heterogeneous Catalysis," *Catal. Rev. Sci. Eng.*, **3**, 71 (1991).

Sahimi, M., "Diffusion-Controlled Reactions in Disordered Porous Media—I. Uniform Distrubutions of Reactants," *Chem. Eng. Sci.*, **43**, 2981 (1988).

Sahimi, M., G. R. Gavalas, and T. T. Tsotsis, "Statistical and Continuum Models of Fluid-Solid Reactions in Porous Media," *Chem. Eng. Sci.*, **45**, 1443 (1990).

Sheintuch, M., and S. Brandon, "Deterministic Approaches to Problems of Diffusion-Reaction and Adsorption in a Fractal Porous Catalyst," *Chem. Eng. Sci.*, **44**, 69 (1989).

Yang, C., M. A. El-Sayed, and S. L. Suib, "Apparent Fractional Dimensionality of Unranil-exchanged Zeolites and Their Protocatalytic Activity," *J. Phys. Chem.*, **91**, 4440 (1987).

Manuscript received Oct. 8, 1996, and revision received Mar. 4, 1997.